

Total energy differences between SiC polytypes revisited

Sukit Limpijumnong and Walter R. L. Lambrecht

Department of Physics, Case Western Reserve University, Cleveland, OH 44106-7079

(September 13, 2021)

The total energy differences between various SiC polytypes (3C, 6H, 4H, 2H, 15R and 9R) were calculated using the full-potential linear muffin-tin orbital method using the Perdew-Wang-(91) generalized gradient approximation to the exchange-correlation functional in the density functional method. Numerical convergence versus \mathbf{k} -point sampling and basis set completeness are demonstrated to be better than 1 meV/atom. The parameters of several generalized anisotropic next-nearest-neighbor Ising models are extracted and their significance and consequences for epitaxial growth are discussed.

PACS: 71.20.Nr, 71.15.Nc, 73.20.Dx

I. INTRODUCTION

Despite many years of study the origin of polytypism in SiC is still not completely understood. A much debated question is whether polytypism is a manifestation of kinetic factors during growth or whether polytypes should be viewed as distinct (possibly metastable) thermodynamic phases with a specific stability range of external parameters (such as pressure, temperature). In a thermodynamic approach to the problem, the most important quantities are the total free energy differences between the various polytypes. A major contribution to the latter is the energy difference at zero temperature. Vibrational entropy contributions at higher temperature were discussed by Heine et al.^{1,2} and Zywietz et al.³ Several groups have performed first-principles local density functional calculations of these energy differences using the norm-conserving pseudopotential plane wave method.⁴⁻⁸ However, there are significant discrepancies between the results of various calculations for these energy differences, which are of order of a few meV/atom or less. More seriously, the three more recent calculations appear to invalidate some of the important conclusions drawn from these calculations by the early work of Heine et al.¹

Heine et al.¹ discussed the relative energy of polytypes in terms of a generalized anisotropic next-nearest-neighbor Ising (ANNNI) spin model in which the energy of a given polytype (per atom) is written as

$$E = E_0 - \frac{1}{N} \sum_{i,n} J_n \sigma_i \sigma_{i+n}, \quad (1)$$

in which N is the number of layers in the system, a “spin” $\sigma_i = \pm 1$ is associated with each (close packed) SiC double layer such that parallel spins represent a locally cubic stacking and antiparallel spins represent a locally hexagonal stacking. The parameters J_n represent the interlayer interaction between successively farther removed layers and E_0 is a common energy reference. In terms of this model truncated beyond $n = 3$ the energies of some of the polytypes of interest are given in column 2 of Table I. According to Heine et al.¹, what distinguishes SiC from other semiconductors, and leads to the multitude of stacking arrangements constituting polytypism, is that $J_1 \cong -2J_2 > 0$ (with $J_n \ll J_{1,2}$ for $n > 2$). For this special ratio of J_1/J_2 , a multi-phase degeneracy point occurs in the ANNNI model corresponding to all phases consisting of successive bands of 2 or 3 parallel spins (which in the following we will call “2-3 banded” polytypes). This would explain the relatively frequent occurrence of polytypes such as 6H (which is $\langle 3 \rangle$ in Zhdanov notation⁹ indicating that it consists of bands of 3 parallel spins), 4H or $\langle 2 \rangle$, 15R or $\langle 32 \rangle$, in contrast to polytypes such as 8H or $\langle 4 \rangle$, 10H or $\langle 5 \rangle$, and 2H or $\langle 1 \rangle$ which are rather rare. Surprisingly, recent calculations⁶⁻⁸ found that $J_1 < |J_2|$, a condition very far away from the multi phase degeneracy point. Secondly, in some of these results,^{6,7} the energy difference $E_{2H} - E_{3C}$ is found to be smaller than the energy difference between 3C and any of the other low energy polytypes. This makes it difficult to understand why 2H is such a rare polytype.

The purpose of the present paper is to systematically re-evaluate these energy differences of polytypes including some new ones and to discuss the meaning of the ANNNI model parameters in the light of these results. Since the accuracy is a crucial matter here, we next discuss the computational method and associated convergence parameters in some detail.

II. COMPUTATIONAL METHOD AND CONVERGENCE TESTS

The computational method employed is the full-potential linear muffin-tin orbital method as implemented by Methfessel¹⁰ and van Schilfgaarde¹¹. The total energy is calculated using the density functional method using the generalized gradient approximation (GGA) for the exchange-correlation energy of Perdew and Wang (PW).¹² For the $E_{2H} - E_{3C}$ energy difference, which is of particular concern below, we verified that other exchange-correlation functionals, such as the Langreth-Mehl GGA¹³ and the Ceperley-Alder¹⁴ and Hedin-Lundqvist¹⁵ parametrizations of the local density approximation yield results which do not differ by more than 1 meV/atom from those for the PW-GGA adopted in the rest of this paper.

In all results presented below, we used the ideal structures but relaxed the total energies with respect to volume. All polytypes were found to closely obey the expected relation $a_h = a_c/\sqrt{2}$ and a_c was found to be 4.33 Å, within 1 % of the experimental value. To check the uncertainties introduced by using ideal structures, we performed relaxations for 2H-SiC. We found $c/a = 1.644$, i.e. slightly larger than the ideal ratio $c/a = \sqrt{8/3} = 1.633$ in good agreement with experiment,¹⁶ which gives $c/a = 1.641$. We obtain $u = 0.3745$ which is very close to the ideal value of $3/8$. The important point is that the total energy per atom in 2H was reduced by only 0.6 meV/atom by relaxation of the structure. In the above calculation, an intra cell parameter u relaxation was performed for each c/a . This energy lowering is consistent with the value estimated from the elastic constants for a distortion from the minimum energy $c/a = \eta$ to the ideal c/a , given by $\Delta E = (1/9)(\delta\eta/\eta)^2\Omega[C_{33} - 2C_{13} + (C_{11} + C_{12})/2]$, in which Ω is the volume per Si-C pair. This expression equals 0.56 meV/atom using the elastic constants given in Ref. 17. Since other polytypes of type $2nH$ are found experimentally to have c/a values closer to the ideal value of $n\sqrt{8/3}$, 2H is the extreme case and places an upper limit on the errors introduced by using ideal structures. The effect of internal cell structural parameters is even an order of magnitude lower. From the TO-phonon frequency in SiC of 23 THz,¹⁷ we can estimate the force constant k for the Si-C bondlength distortions to be 18 eV/Å². Thus the change in energy per bond related to a bond-length change of $\delta l = (\delta u)c$ is $\Delta E = (1/2)k(\delta l)^2$. This gives only 0.03 meV/atom for our calculated δu in good agreement with our direct calculation. High precision theoretical determinations of the atomic relaxations were reported by Käckel et al.⁷ They confirm that the bond lengths differ by less than 0.3 % from the ideal bond length which according to the above estimate would give at most 0.14 meV/atom for the relaxation energy. As far as atomic relaxation effects on the total energies is concerned, our results differ substantially from theirs. In their results without atomic relaxations or cell-shape relaxations, 2H lies about 8 meV/atom above 3C and the energy of the polytypes increases monotonically with hexagonality. They find the internal cell atomic relaxations to have a marked effect on all hexagonal polytypes resulting in a lower energy than 3C for 6H and 4H and a substantial reduction of the 2H to 3C energy difference to only 1 meV/atom. This implies that the relaxations would produce relative changes of 3, 4, and 7 meV/atom for 6H, 4H and 2H respectively. This is inconsistent with the above estimates based on elastic and force constants and with our explicit calculations. The origin of this discrepancy is not entirely clear. However, the comparison between their relaxed and unrelaxed energies is complicated by their use of different \mathbf{k} point sets for the two calculations. As will be shown below, converged Brillouin zone integrations are an important requirement for drawing conclusions about polytype energy differences. As we will show below, we find 6H and 4H to have lower energy than 3C without cell shape or internal position relaxations.

With respect to self-consistency, all total energies were converged to better than 0.1 meV/atom. The contributions to the total charge density from each angular momentum component were converged to a root mean square error less than 10^{-4} electron. Within FP-LMTO, the wave functions are expanded in an extended basis set of muffin-tin orbitals with different spatial decay constants (i.e spherical Hankel envelope function exponents κ). Fig. 1 shows results for different basis sets for the $E_{2H} - E_{3C}$ energy difference and the individual cohesive energies of E_{2H} and E_{3C} . The notation for the basis set is illustrated as follows: dps means up to d orbitals for the first $\kappa = -0.05$ Ry, up to p for second $\kappa = -1$ Ry and one s orbital for the third $\kappa = -2.3$ Ry. The unfilled bars in the bottom graph give E_{2H} , the filled ones E_{3C} . The top graph gives their energy difference in meV/atom. The dashed lines indicate the corresponding information for the same basis sets with f -orbitals added for the first κ . We can see that the contributions of each orbital to the total cohesive energies are several 10 meV and that increasing the basis set decreases the energy. Adding the f -orbitals makes about a -30 meV contribution independently of which basis set they are added to. The third κ d -orbital contributes only about -7 meV to the total energy. The most important point is that the polytype energy difference is stable at 2.4 ± 0.3 meV/atom for the four most complete basis sets considered. Adding empty sphere orbitals s and p and second κ s to the ddp basis set changed the energies by only -8 meV and is thus also considered ineffective. For polytypes with many atoms per unit cell, the calculations with the basis sets larger than fdp tend to become unstable. If the basis set is very close to completeness, slight numerical errors can make the basis set appear to be overcomplete or linearly dependent. The optimal basis set is thus considered to be fdp and used systematically for the other polytypes.

The integrations over the interstitial region are done using an auxiliary set of spherical Hankel functions times

spherical harmonics for expansion of products of two Hankel functions. These expansions are cut-off at $l_{max} = 6$. We found that this cut-off is necessary to make the results stable and independent of the sphere radii choice. The empty spheres were chosen to be nearly touching with two empty spheres equal in size to the atomic spheres (Si and C being chosen equal) in each cubic stacking double layer unit and a large ($1.134 s_{atom}$) and small empty sphere ($0.666 s_{atom}$) in each hexagonal unit. The large spheres occupy the empty channel in the wurtzite structure. That is, if atoms are taken to sit in A and B positions in the basal plane, the large empty spheres occupy the C positions in the plane at a height halfway between the bonding Si and C atoms in the A position. The small spheres occupy the sites halfway between the Si and C atoms opposite to the nearest neighbor Si-C bond along the c -axis. In cubic SiC, the spheres occupy about 68 % of the unit cell volume. In 2H they occupy 63 % of the volume and in other polytypes the filling is in between these values in proportion to the degree of hexagonality (i.e. the ratio of the number of hexagonally stacked layers h to the total (i.e hexagonal and cubic c) number of layers $h/(h + c)$).

The next convergence issue to consider is the Brillouin zone integration. The Monkhorst-Pack¹⁸ special \mathbf{k} -points sampling technique is used with the number of divisions along reciprocal lattice vectors in the basal plane equal to N and along the c -axis equal to M . For longer polytypes (along the c -axis), one needs fewer divisions M along the c -axis. Rather than picking exactly equivalent sets for each polytype, and thus counting on error cancellation, we picked M large enough to ensure absolute convergence. For 2H, we used $M = N$ and for longer polytypes we reduced to $M = N/2$ for the larger N values. Fig. 2 shows the results for various polytypes as a function of N . The quantity shown is $\Delta E_P(N) - \Delta E_P(\infty)$, where $\Delta E_P(N) = E_P(N) - E_{3C}$, the energy difference for a given polytype P from the absolutely converged value of E_{3C} calculated with $N = M = 10$, and the value of $E_P(\infty)$ is estimated by extrapolation so as to ensure that all results fall on a universal curve. This clearly shows that the final values $\Delta E_P(\infty)$ are converged to better than 0.5 meV/atom.

III. RESULTS AND DISCUSSION

The converged energy differences of the polytypes with respect to 3C, i.e. $\Delta E_P(\infty)$ as defined in the previous section, are given in column 3 of Table I. They are compared to those of previous calculations in the literature in Fig. 3.

Next, we extract the J_n parameters. Columns 4 and 5 correspond respectively to truncation at $n_{max} = 2$ and $n_{max} = 3$ using the energy differences $E_{2H} - E_{3C}$, $E_{4H} - E_{3C}$ as input in the first case and additionally $E_{6H} - E_{3C}$ in the latter case. The other polytypes then allow for a check of the consistency of this model. We find the J_n parameters J_1 and J_2 , as listed in Table I, to be nearly independent of whether or not J_3 is included. Furthermore, we find $J_1 > |J_2|$.

Our results are somewhat closer to those of Heine et al.¹ than the other recent results, particularly that E_{2H} is higher above E_{3C} by an amount significantly larger than the other polytype energy differences. Also, we find the various 2-3 banded polytypes to be closer to each other than in the other calculations. Nevertheless, our results are far from the multiphase degeneracy point $J_1 = -2J_2$. As Heine pointed out, the energy of a twin boundary, i.e. the energy cost of a boundary between all up-spin all down-spin cubic half crystals is given by

$$E_{twin} = 2(J_1 + 2J_2). \quad (2)$$

According to Heine et al., this is nearly zero and hence explains why many twin boundaries in an otherwise cubically stacked crystal are likely to occur. With our present values of the J_n parameters, the energy cost of a twin is *negative*. This implies that twins are even more favorable than in Heine's model. Hence, there is no contradiction at all with the observation of a predominance of 2-3 banded polytypes.

Consistently with other recent work we find 4H to have lower energy than 6H. In the FP-LMTO calculations, we find 15R as lowest energy polytype. In the ANNNI model we find 15R to lie in between 4H and 6H with 4H the lowest energy polytype. This is slightly more expected since 15R is intermediate in character between 4H and 6H. This discrepancy, which is smaller than 0.5 meV, may be beyond the accuracy of our FP-LMTO calculations in view of the fact that the computational convergence is most challenging for the largest polytype. As expected, the hypothetical^{19,20} 9R polytype with a high degree of hexagonality (66%) is found to have higher energy than 3C but lower than 2H.

The ANNNI model appears to somewhat underestimate the energy of 9R. This suggests that other terms in the effective Hamiltonian may be required. A term

$$K \sum_i \sigma_i \sigma_{i+1} \sigma_{i+2}, \sigma_{i+3}, \quad (3)$$

was suggested by Cheng et al.⁴ The additional energy for each polytype due to this term is given in column 5 in Table I. Column 6 shows that this term allows us to fit 9R exactly without affecting the energy of 15R significantly.

We next consider the predictions of the model for a few other polytypes. Another polytype of high hexagonality (80 %) was recently considered²⁰ and labeled 15R' or $\langle 1112 \rangle$. Its energy within the ANNNI model is given in the bottom section of Table I. As expected, it is higher in energy than 9R but still lower than 2H. We do not interpret this as an indication that these particular periodic stacking arrangements are more likely (because they seem excessively complicated) but rather as an indication that a high density of stacking faults is likely to occur in 2H. For any $2nH$ polytype with $n \geq 3$ the energy difference from 3C can be written as $\frac{2}{n}(J_1 + 2J_2 + 3J_3 - 2K)$. This shows that for $n \rightarrow \infty$, it will approach zero as expected since 3C corresponds to ∞H , but only very slowly. In fact, the energies of 8H and 10H are seen in Table I to be still rather close to those of the 2-3 banded polytypes, consistent with the fact that these polytypes have indeed been observed.

As for the phonon contributions to the free energy, (here denoted F_P) we note that Heine et al.¹ obtain a result which is the opposite of that found by Zywiets et al.³, namely $F_{4H} > F_{6H}$ and increasing with temperature. This tends to stabilize 6H at high temperatures whereas Zywiets et al.³ find 4H to become even more stabilized at higher than at lower temperatures without affecting the polytype free energy ordering. We note that with our calculated $E_{4H} - E_{6H}$ at zero temperature, and Heine's values for the phonon contribution, the transition from 4H stability to 6H stability is predicted to occur above 8000 K, i.e. well above the melting temperature of SiC. With Zywiets et al.'s phonon contributions, no stabilization of 6H will ever occur. We conclude that either way, there is no substantial evidence from the calculations that the polytypes would have a well-defined temperature stability region. We think it is much more likely that the slightly different tendencies for 4H and 6H growth in dependence on the growth temperature is due to kinetic factors. In fact, these experimental tendencies have not unequivocally been established.

Heine et al.²¹ also argued that the 3C dominance in epitaxial growth could be explained by assuming that only the surface layer stacking is determined by the equilibrium energy condition but that the stacking is not subsequently re-arranged after the layer is buried into the growing crystal. Since the energy difference for adding one surface layer to a substrate with opposite spin of the top layer as opposed to equal spin is $J_s = 2(J_1 \pm J_2)$, with \pm depending on whether the next layer down has equal or opposite spin, cubic stacking is always favored as long as $J_1 + J_2 > 0$. As in Heine et al.'s results, and in contrast to other recent results,⁶⁻⁸ our present results satisfy this requirement although only barely so. Of course, we caution that these interlayer interactions may change at a surface. If $J_1 + J_2 < 0$, on the other hand, a 4H stacking would always be preferred as can easily be checked by following the same argument as given by Heine. The point is that second layer interactions, which are "antiferromagnetic" are then dominant. Thus, if we start from two equal spins in the top layers, the next growing layer must have opposite spin. The new surface ends then in two opposite spins and the following layer must have the same spin as the one last deposited, after which the cycle repeats. This is inconsistent with experimental observations. Independent nucleations on large terraces tend to have the 3C structure, which usually is accompanied by a large amount of so-called double positioning boundaries.

Given that the preference for cubic stacking during growth is so small, the question arises whether this is really relevant. To address this question, we must consider size effects of the growing fragments. For a 2D island of N_i spins (or SiC units), the energy differences for being in a cubic or hexagonal stacking on top of a substrate should be of order $N_i J_s$. This implies that up to $N_i J_s \approx k_B T_G$ with T_G the growth temperature and k_B Boltzman's constant, or for a typical growth temperature of 1500K, and using $J_s = 0.3$ meV/SiC unit, up to $N_i \leq 600$, there should be virtually no distinction in energy between either stacking. On the other hand, islands will definitely tend to be of a well-defined spin. This is because a lateral spin-boundary corresponds ultimately to a defect such as an incoherent twin boundary. The energy of the latter is typically of the order of several eV/atom.²² This is because there are serious disruptions of the tetrahedral bonding associated with such boundaries, including wrong bonds (C-C or Si-Si) and possibly dangling bonds. Thus, atoms migrating on the surface will have a strong tendency to adjust their spin (i.e. stacking with respect to the underlying layers) to that of the growing island to which they are attaching. This explains why well-defined polytype structures can evolve even if the growth does not occur in a strict layer-by-layer fashion in spite of the energy differences for different stacking for each atom being much smaller than the growth temperature. Only for islands of the above defined size, which corresponds to ~ 10 nm in diameter, one expects that the interactions with underlying layers become relevant. A predominance of cubic stackings with respect to the underlying layers assumes that such 2D islands can still adjust their stacking position by moving as a whole. Although this might seem to require overcoming a significant energy barrier, motion of islands might occur by a 2D dislocation motion. In the above estimate, we used $J_s = 2(J_1 + J_2)$ neglecting J_3 and K interactions. We also assumed growth on a cubic substrate and renormalized to energies per SiC unit rather than per atom. For growth on other polytype substrates or when including J_3 and/or K , the interaction J_s becomes somewhat larger and hence the critical island size somewhat smaller, but the general argument does not change. Even though a preference for cubic stacking can thus be rationalized, a certain number of double positioning boundaries are expected because some islands of opposite spin may become trapped in an initially unfavorable stacking due to the randomness of the initial nucleation events. A step-flow growth mechanism seems to be the only plausible mechanism for stabilizing other polytypes during epitaxial

growth and depends crucially on the sizes of the terraces and the surface diffusion (hence growth temperature).²³

IV. CONCLUSIONS

In conclusion, we have carefully re-evaluated the zero-temperature energy differences between polytypes of SiC using well-converged all-electron density functional calculations. We find that the ANNNI model with up to second nearest neighbor layer interactions already provides a good description of the polytype energy differences with slight improvements being obtained by including a third layer interaction and a 4-spin term. Even though the values for J_1 , J_2 do not correspond to the multi-phase degeneracy point, the predominance of polytypes of narrow bands of cubic stacking (typically 2-3 banded) can readily be explained by the fact that $J_1 > 0$ and the twin boundary energy cost is negative. Our results agree closer with Heine et al.'s¹ work than other recent calculations, in the sense that we obtain $J_1 > |J_2|$, the 2-3 banded polytype energies closer to each other and the 2H energy significantly higher than that of 3C. We stress that this is not due to our neglect of relaxations because the latter were shown to be at most 0.6 meV/atom. We nevertheless find the energies of 4H and 6H to differ substantially enough to preclude a well-defined temperature stability region for each polytype when using literature data for the vibrational free energy contributions. This suggests that polytypes are kinetically determined metastable phases rather than true thermodynamic phases. Some consequences for epitaxial growth were discussed. In particular, we extended Heine et al.'s arguments concerning the tendency for 3C growth to occur if only equilibrium of the top-surface layer is required by considering the island size effects. We also showed that for $J_1 < |J_2|$, 4H would always be stabilized, which is inconsistent with experiment.

We thank B. Segall for useful discussions. This work was supported by NSF DMR-95-29376.

-
- ¹ V. Heine, C. Cheng, G. E. Engel, and R. J. Needs, in *Wide Band Gap Semiconductors*, ed. T. D. Moustakas, J. I. Pankove, and Y. Hamakawa, Mat. Res. Soc. Symp. Proc. Vol. 242, p. 507 (Mater. Res. Soc., Pittsburgh, 1992); V. Heine, C. Cheng, and R. J. Needs, Mater. Sci. and Eng. B, **11**, 55 (1992).
- ² C. Cheng, V. Heine, and I. L. Jones, J. Phys. Condens. Matter **2**, 5097 (1990).
- ³ A. Zywietz, K. Karch and F. Bechstedt, Phys. Rev. B **54**, 1791 (1996).
- ⁴ C. Cheng, R. J. Needs, and V. Heine, J. Phys. C **21**, 1049 (1988).
- ⁵ C. Cheng, V. Heine, and R. J. Needs, J. Phys. Condens. Matter **1**, 5115 (1990).
- ⁶ C. H. Park, B.-H. Cheong, K.-H. Lee, and K. J. Chang, Phys. Rev. B **49**, 4485 (1994).
- ⁷ K. Käckell, B. Wenzien, and F. Bechstedt, Phys. Rev. B **50**, 17037 (1994).
- ⁸ K. Karch, G. Wellenhofer, P. Pavone, U. Rössler, and D. Strauch, in *Proc. 22nd Int. Conf. Phys. Semicond.*, edited by D. Lockwood (World Scientific, Singapur, 1995), p. 401.
- ⁹ G. S. Zhdanov *C. R. Academ. Sci. USSR* **48**, 43 (1945).
- ¹⁰ M. Methfessel, *Phys. Rev. B* **38** 1537 (1988).
- ¹¹ We use a modified version of the program provided by M. van Schilfhaarde, private communication.
- ¹² J. P. Perdew, in *Electronic Structure of Solids '91*, edited by P. Ziesche and H. Eschrich (Akademie Verlag, Berlin, 1991), p. 11; J. P. Perdew, K. Burke, and M. Ernzerhof, Phys. Rev. Lett. **77**, 3865 (1996).
- ¹³ D. C. Langreth and M. J. Mehl, Phys. Rev. B **28**, 1809 (1983).
- ¹⁴ D. M. Ceperley and B. J. Alder, Phys. Rev. Lett. **45**, 566 (1980); J. P. Perdew and A. Zunger, Phys. Rev. B **23**, 5048 (1981).
- ¹⁵ L. Hedin and B. I. Lundqvist, J. Phys. C **4**, 2064 (1971).
- ¹⁶ R. W. G. Wyckoff, *Crystal Structures*, 2nd ed. (Interscience, New York, 1964), Vol. 1, p. 113.
- ¹⁷ W. R. L. Lambrecht, B. Segall, M. Methfessel, and M. van Schilfhaarde, Phys. Rev. B **44**, 3685 (1991).
- ¹⁸ H. J. Monkhorst and J. D. Pack, Phys. Rev. B **13**, 5188 (1976).
- ¹⁹ A trigonal symmetry polytype 9T was reported by Z. Inoue, S. Sueno, T. Tagai, and Y. Inomata, J. Cryst. Growth **8**, 179 (1983) but corresponds to Zhdanov notation ⟨63⟩; polytypes other than 2H containing 1 in their Zhdanov symbol such as 9R, 15R' were never observed according to P. Krishna, R. C. Marshall, and C. E. Ryan, J. Cryst. Growth **8**, 129 (1971) and Z. Inoue, J. Mater. Sci. **17**, 3189 (1982).
- ²⁰ W. R. L. Lambrecht, S. Limpijumngong and B. Segall, in *Silicon Carbide and Related Materials*, edited by Shin-ichi Nakashima, Hyroyuki Matsunami, Sadafumi Yoshida, and Hiroshi Harima, Inst. Phys. Conf. Series No. 142, (IOP Publishing, Bristol, 1996), p. 263.
- ²¹ V. Heine, C. Cheng, and R. J. Needs, *J. Am. Ceram. Soc.* **74**, 2630 (1991).
- ²² M. Kohyama and R. Yamamoto, in *Diamond, SiC and Nitride Wide Bandgap Semiconductors*, ed. C. H. Carter, Jr., G. Gildenblat, S. Nakamura, and R. J. Nemanich, Mater. Res. Soc. Symp. Proc. Vol. 339, p.9 (MRS, Pittsburgh 1995).

²³ H. Matsunami and T. Kimoto in *Diamond, SiC and Nitride Wide bandgap Semiconductors*, ed. C. H. Carter, Jr., G. Gildenblat, S. Nakamura, and R. J. Nemanich, *Mater. Res. Soc. Symp. Proc.* Vol. **339**, p. 369 (MRS, Pittsburgh, 1994).

TABLE I. Energy difference $\Delta E_P = E_P - E_{3C}$ for various polytypes P in meV/atom

P	ANNNI	FP-LMTO	$n_{max} = 2$ ^a	$n_{max} = 3$ ^b	K -term	$n_{max} = 3, +K$ ^c
2H	$2J_1 + 2J_3$	2.7	2.7	2.7	0	2.7
4H	$J_1 + 2J_2 + J_3$	-1.2	-1.2	-1.2	0	-1.2
6H	$\frac{2}{3}J_1 + \frac{4}{3}J_2 + 2J_3$	-1.05	-0.08	-1.05	$-\frac{4}{3}K$	-1.05
9R	$\frac{4}{3}(J_1 + J_2)$	1.0	0.1	0.3	$-\frac{4}{3}K$	1.0
15R	$\frac{4}{5}(J_1 + 2J_2 + 2J_3)$	-1.5	-1.0	-1.1	$-\frac{4}{5}K$	-1.1
15R [†]	$\frac{4}{5}(2J_1 + J_2 + J_3)$		1.1	1.3	$-\frac{4}{5}K$	1.6
8H	$\frac{1}{2}(J_1 + 2J_2 + 3J_3)$		-0.6	-0.8	$-K$	-0.9
10H	$\frac{2}{5}(J_1 + 2J_2 + 3J_3)$		-0.5	-0.6	$-\frac{4}{5}K$	-0.7

^aUsing $J_1 = 1.350$, $J_2 = -1.285$, $J_3 = 0$, extracted from first two polytypes

^bUsing $J_1 = 1.528$, $J_2 = -1.285$, $J_3 = -0.177$ meV/atom, extracted from first three polytypes

^cUsing $J_1 = 1.781$, $J_2 = -1.275$, $J_3 = -0.431$, $K = -0.244$ meV/atom extracted from first four polytypes

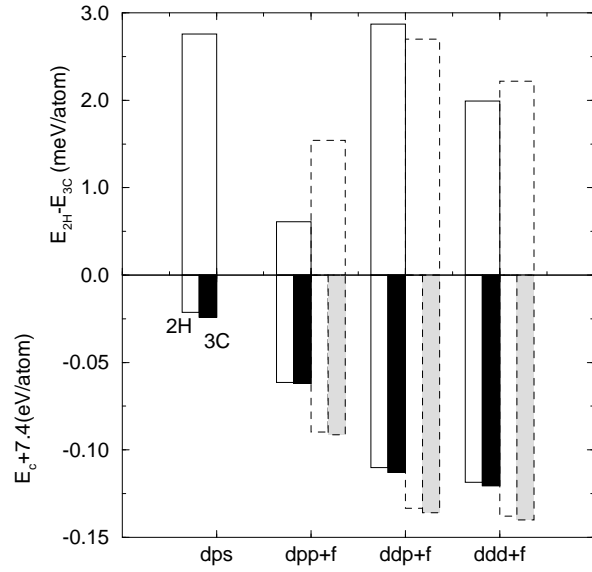


FIG. 1. Basis set convergence of $E_{2H} - E_{3C}$. Bottom graph shows cohesive energies of 2H and 3C as open and filled bar graphs with various basis sets as indicated. Top graph shows $E_{2H} - E_{3C}$. Dashed (full) lines are results for which f -orbitals are (not) included.

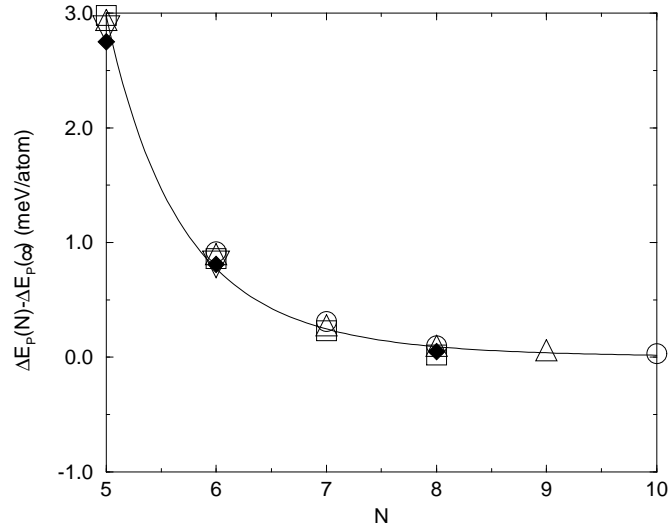


FIG. 2. Brillouin zone sampling convergence. N is the number of divisions along the two basal plane reciprocal lattice vectors. Circles: 2H, squares: 4H, filled diamonds 6H, upward triangles 9R, downward triangle 15R. The full line curve is a powerlaw fit $e^{13}N^{-7.4}$. The values of $\Delta E_P(\infty)$ are given in Table I.

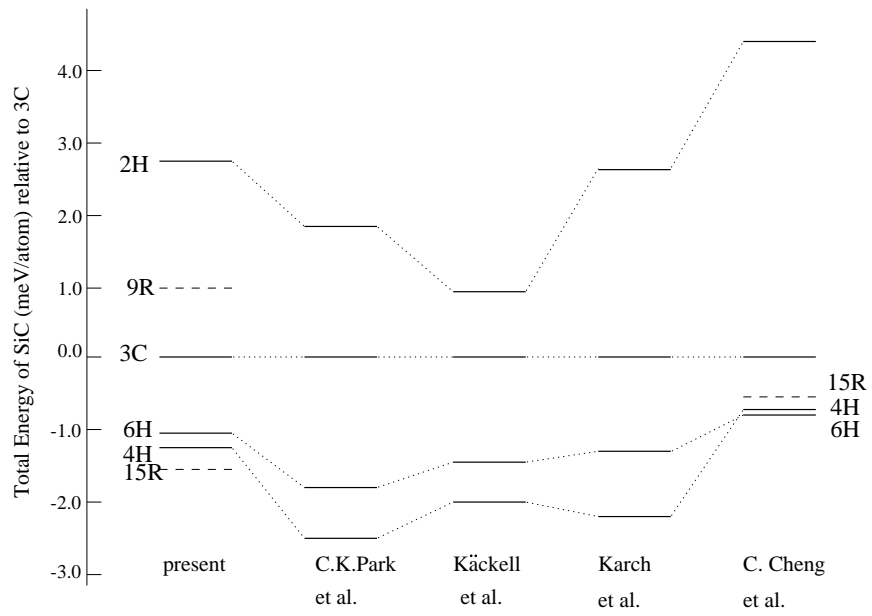


FIG. 3. Energy differences between various polytypes: comparison with other calculations.